

# DNA polymerase $\zeta$ generates tandem mutations in immunoglobulin variable regions

Huseyin Saribasak,<sup>1</sup> Robert W. Maul,<sup>1</sup> Zheng Cao,<sup>1</sup> William W. Yang,<sup>1</sup> Dominik Schenten,<sup>2</sup> Sven Kracker,<sup>2</sup> and Patricia J. Gearhart<sup>1</sup>

<sup>1</sup>Laboratory of Molecular Biology and Immunology, National Institute on Aging, National Institutes of Health, Baltimore, MD 21224

<sup>2</sup>Immune Disease Institute, Harvard Medical School, Boston, MA 02115

**Low-fidelity DNA polymerases introduce nucleotide substitutions in immunoglobulin variable regions during somatic hypermutation. Although DNA polymerase (pol)  $\eta$  is the major low-fidelity polymerase, other DNA polymerases may also contribute. Existing data are contradictory as to whether pol  $\zeta$  is involved. We reasoned that the presence of pol  $\eta$  may mask the contribution of pol  $\zeta$ , and therefore we generated mice deficient for pol  $\eta$  and heterozygous for pol  $\zeta$ . The frequency and spectra of hypermutation was unaltered between  $Pol\zeta^{+/-} Pol\eta^{-/-}$  and  $Pol\zeta^{+/-} Pol\eta^{-/-}$  clones. However, there was a decrease in tandem double-base substitutions in  $Pol\zeta^{+/-} Pol\eta^{-/-}$  cells compared with  $Pol\zeta^{+/+} Pol\eta^{-/-}$  cells, suggesting that pol  $\zeta$  generates tandem mutations. Contiguous mutations are consistent with the biochemical property of pol  $\zeta$  to extend a mismatch with a second mutation. The presence of this unique signature implies that pol  $\zeta$  contributes to mutational synthesis in vivo. Additionally, data on tandem mutations from wild type,  $Pol\zeta^{+/-}$ ,  $Pol\zeta^{-/-}$ ,  $Ung^{-/-}$ ,  $Msh2^{-/-}$ ,  $Msh6^{-/-}$ , and  $Ung^{-/-} Msh2^{-/-}$  clones suggest that pol  $\zeta$  may function in the MSH2-MSH6 pathway.**

## CORRESPONDENCE

Patricia J. Gearhart:  
gearhartp@mail.nih.gov

Abbreviations used: AID, activation-induced deaminase; CSR, class switch recombination; pol, polymerase; SHM, somatic hypermutation; UNG, uracil DNA glycosylase

Somatic hypermutation (SHM) generates nucleotide substitutions in immunoglobulin variable (V) regions at a frequency of  $10^{-2}$ – $10^{-3}$  mutations per base pair (bp), which far exceeds the frequency of spontaneous mutation. SHM is initiated by activation-induced deaminase (AID), which is targeted to V regions by an unknown mechanism. AID transforms cytosine into mutagenic uracil in DNA (Maul et al., 2011), which can be recognized by DNA repair proteins uracil DNA glycosylase (UNG) to remove the uracil leaving an abasic site, or MSH2-MSH6 to generate a gap in the DNA (Maul and Gearhart, 2010). However, the sheer number of AID-generated uracils appears to overwhelm the error-free base excision and mismatch repair

pathways (Saribasak et al., 2011), and the abasic sites and gaps then become substrates for low-fidelity DNA polymerases. Low-fidelity polymerases were originally described for their ability to replicate over DNA lesions, such as base adducts, cyclobutane pyrimidine dimers, and abasic sites. Although these lesions inhibit the replicative and repair polymerases, low-fidelity polymerases have the unique ability to insert nucleotides opposite lesions and to extend from mismatched termini. However, their inherent low fidelity causes them to be remarkably promiscuous when copying undamaged DNA, making them candidates for SHM. It is not fully understood how these polymerases are recruited to the immunoglobulin loci in place of their high-fidelity counterparts, although differential modifications of PCNA have been shown to coordinate some of the events (Langerak et al., 2007; Roa et al., 2008).

H. Saribasak and R.W. Maul contributed equally to this paper. H. Saribasak's present address is Dept. of Basic Medical Sciences, Sifa University School of Medicine, Izmir, Turkey. D. Schenten's present address is Dept. of Immunobiology, Yale University School of Medicine, New Haven, CT 06520. S. Kracker's present address is Institut National de la Santé et de la Recherche Médicale U768, Hôpital Necker Enfants Malades, F-75015 Paris, France.

© 2012 Saribasak et al. This article is distributed under the terms of an Attribution-Noncommercial-Share Alike-No Mirror Sites license for the first six months after the publication date (see <http://www.rupress.org/terms>). After six months it is available under a Creative Commons License (Attribution-Noncommercial-Share Alike 3.0 Unported license, as described at <http://creativecommons.org/licenses/by-nc-sa/3.0/>).

Many DNA polymerases have been examined for their role in SHM, with most of them belonging to the Y family of polymerases that exhibit lower fidelity than the other polymerases (Seki et al., 2005). Their involvement is demonstrated by the altered frequency and/or spectra of mutations in mice that are deficient for the polymerases. However, in most cases, the frequency is unchanged because of intense selection in vivo for B cells expressing antibodies with mutations giving high affinity for antigen. Instead, changes in the types of mutations have allowed identification of relevant polymerases based on their intrinsic signature of substitutions, as defined by their enzymatic properties. SHM in wild-type mice is characterized by equal mutations of G:C and A:T bp, with transitions outnumbering transversions. The predominant category of G:C to A:T transitions, which comprises 60% of all G:C mutations, is likely caused by replication past uracil by any of the DNA polymerases (Petersen-Mahrt et al., 2002). Rev1 is the major polymerase that produces G:C to C:G transversions, because its property as a deoxycytidyl transferase is to insert C opposite the abasic site that is produced by removal of uracil by UNG (Jansen et al., 2006). Polymerase (pol)  $\eta$  is the major polymerase that produces mutations of A:T bp, because *Pol $\eta$ <sup>-/-</sup>* cells have a 60% decrease in A:T mutations (Zeng et al., 2001). Pol  $\kappa$  can generate half of the residual A:T mutations in the absence of pol  $\eta$  (Faili et al., 2009). Pals  $\iota$  (McDonald et al., 2003) and the A-family pol  $\theta$  (Martomo et al., 2008) have also been examined, but there is no clear evidence of a change in spectra in their absence.

The B family DNA pol  $\zeta$  is up-regulated in replicating cells, including germinal center B cells (Zeng et al., 2001), but its role in SHM has been difficult to analyze because mice deficient for the enzyme are not viable (Bemark et al., 2000; Esposito et al., 2000; Wittschieben et al., 2000). Several studies in cell lines and transgenic mice showed that reduction of pol  $\zeta$  by knockdown or antisense techniques lowered the frequency of SHM but did not change the spectra

(Diaz et al., 2001; Zan et al., 2001). Recently, Schenten et al. (2009) generated mice that conditionally knocked out Rev3, the catalytic subunit of pol  $\zeta$ , in B cells. In these mice, half of the B cells were deficient for pol  $\zeta$ , and they had a lower frequency of SHM but no change in the types of substitutions. The authors concluded that the lower frequency was simply caused by a decreased rate of cell division and reduced germinal center formation, suggesting that pol  $\zeta$  did not play a direct role in SHM.

These previous studies indicate that either pol  $\zeta$  is not used during SHM, or it has only a modest role that may be masked by other low-fidelity polymerases. Therefore, we examined mice deficient for the dominant pol  $\eta$  that contained one or two alleles encoding pol  $\zeta$ , to see if pol  $\zeta$  plays a more visible role in the absence of pol  $\eta$ . Because pol  $\zeta$  is comprised of two subunits, the catalytic Rev3 protein and the noncatalytic Rev7 protein, we used mice with a targeted allele of Rev3 (Wittschieben et al., 2010) and crossed them with pol  $\eta$ -deficient mice.

## RESULTS AND DISCUSSION

### Combined deficiencies of pols $\zeta$ and $\eta$ did not alter cell division, class switch recombination (CSR), and SHM

We have previously shown that *Pol $\eta$ <sup>-/-</sup>* mice had a normal frequency of germinal center B cells and CSR (Martomo et al., 2005). In this study, we tested if *Pol $\eta$ <sup>-/-</sup>* cells with one allele of pol  $\zeta$  behaved differently than cells with two alleles. To confirm that pol  $\zeta$  is down-regulated in the heterozygous cells, mRNA levels were measured by quantitative PCR from B cells. Primers were used that were located within the two deleted exons, 26 and 27, encoding Rev3 on the targeted allele to ensure

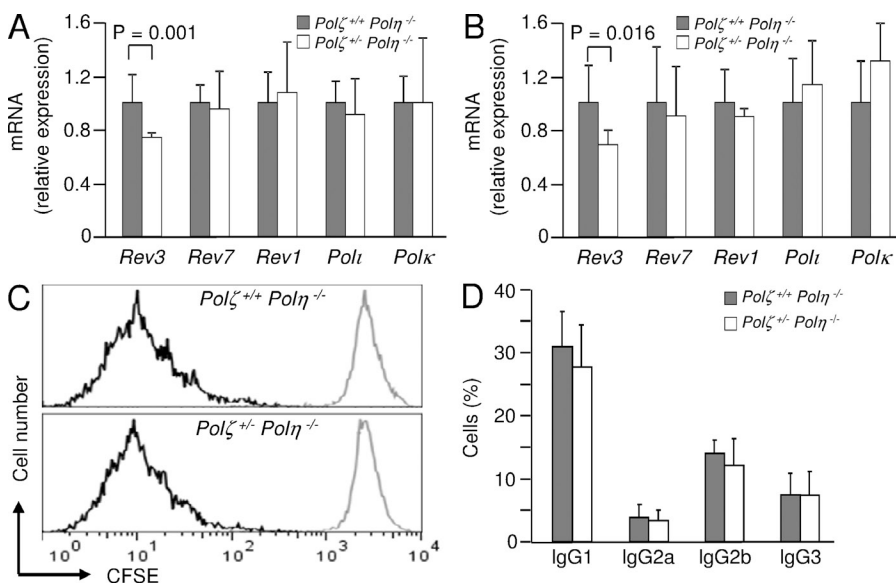


**Figure 1. Normal proliferation and CSR in splenic B cells with different pol  $\zeta$  and pol  $\eta$  genotypes.** mRNA was isolated from resting B cells from untreated mice (A) and germinal center cells from mice immunized with NP<sub>36</sub>-CGG for 14 d (B). *Rev3*, *Rev7*, *Rev1*, *Polt*, and *Polk* mRNA was measured by quantitative RT-PCR. Values are shown relative to  $\beta$ -actin transcripts, and are standardized to the levels in *Pol $\zeta$ <sup>+/+</sup> Pol $\eta$ <sup>-/-</sup>* cells from littermate mice. Error bars depict the SD of values from three independent experiments using one mouse per genotype per experiment. Significance was determined by the two-tailed Student's *t* test. (C) B cells from indicated mice were labeled with CFSE and activated ex vivo with LPS and IL-4 for 3 d. Seven independent experiments were performed using one littermate mouse per genotype per experiment. Representative curves are shown for day 0 (gray) and day 3 (black). (D) B cells were incubated for 4 d with various cytokines and LPS, and expression of the indicated antibody isotypes was measured by flow cytometry. Error bars signify the SD of values from four independent experiments with one to three littermate mice per genotype per experiment.

that we did not detect any mRNA from potential alternatively spliced transcripts. Compared with  $Pol\zeta^{+/+} Pol\eta^{-/-}$  cells, Rev3 transcripts were significantly decreased (25–30%) in  $Pol\zeta^{+/-} Pol\eta^{-/-}$  cells that were either resting (Fig. 1 A;  $P = 0.001$ ) or stimulated in vivo with 4-hydroxy-3-nitrophenyl-acetyl conjugated to chicken  $\gamma$  globulin (NP<sub>36</sub>-CGG) for 14 d (Fig. 1 B;  $P = 0.016$ ). In contrast, there was no change in mRNA encoding Rev7, or in Rev1, a binding partner of pol  $\zeta$ , showing that lower Rev3 levels did not affect these transcripts. There was also no significant change in the levels of pols  $\iota$  and  $\kappa$ , indicating that they did not overcompensate for the reduction in Rev3.

Because complete loss of pol  $\zeta$  in conditional knockout mice caused slower B cell growth (Schenten et al., 2009), we examined  $Pol\zeta^{+/-} Pol\eta^{-/-}$  cells after stimulation with LPS and IL-4 for cell proliferation by CFSE. As shown in Fig. 1 C, haploinsufficiency of pol  $\zeta$  did not affect cell division after 3 d. Pol  $\zeta$  is also recruited to sites of double-strand DNA breaks (Hirano and Sugimoto, 2006), which are key intermediates in CSR. To see if a deficiency of pol  $\zeta$  cripples recombination,  $Pol\zeta^{+/+} Pol\eta^{-/-}$  and  $Pol\zeta^{+/-} Pol\eta^{-/-}$  naive B cells were stimulated for 4 d to induce switching from IgM to different IgG isotypes. Compared with  $Pol\zeta^{+/+} Pol\eta^{-/-}$  cells,  $Pol\zeta^{+/-} Pol\eta^{-/-}$  cells had a slight decrease in recombination to IgG1, IgG2a, and IgG2b, although the numbers were not significantly different (Fig. 1 D). Thus, in contrast to the conditional knockout mouse, which showed a 50% decrease in switching caused by defective nonhomologous end joining (Schenten et al., 2009), the residual pol  $\zeta$  protein in the heterozygous cells was sufficient to permit CSR at normal levels.

To analyze the contribution of pol  $\zeta$  to SHM, we immunized mice with NP<sub>36</sub>-CGG, and isolated germinal center cells 14 d later. SHM was analyzed in the J<sub>H</sub>4 intron downstream of rearranged V<sub>H</sub>J558 genes, and  $Pol\zeta^{+/-} Pol\eta^{-/-}$  clones had a similar mutational frequency and mutations per clone compared with  $Pol\zeta^{+/+} Pol\eta^{-/-}$  clones (Fig. 2, A–C). Analysis of the types of mutations showed no difference between  $Pol\zeta^{+/+} Pol\eta^{-/-}$  and  $Pol\zeta^{+/-} Pol\eta^{-/-}$  clones (Fig. 2 D).

### Identification of a new signature for pol $\zeta$ in SHM: tandem mutations

The ascribed role of pol  $\zeta$  is to extend mismatched primer termini (Lawrence and Maher, 2001) produced by other low-fidelity polymerases when copying past lesions, by adding the correct base (Johnson et al., 2000). However, recent evidence indicates that pol  $\zeta$ , which has an error rate of  $\sim 10^{-3}$ , can also extend mismatches produced by itself or other polymerases with a second mutation, generating tandem double-base mutations (Zhong et al., 2006; Sakamoto et al., 2007). The second mutation occurs at a rate of  $10^{-2}$ , indicating that pol  $\zeta$  frequently inserts incorrect bases when confronted with mismatched termini. Therefore, we examined DNA sequences to see if we could find this signature of pol  $\zeta$  (Fig. S1).

First, we looked at published wild-type sequences (Rada et al., 2002; Martomo et al., 2008; Schenten et al., 2009; Saribasak et al., 2011) to establish the location and spectra of

tandem mutations. The aligned mutational data in 492 bp encoding the J<sub>H</sub>4 intron in Fig. 3 A shows the distribution of 1,811 single mutations and their location relative to the 6 WGCW (W = A/T) hotspots in the sequence. As seen in Fig. 3 B, the distribution of 50 pairs of tandem mutations resembled the location of single mutations, and only 18% of them occurred in WGCW motifs.

Second, to see if the distribution of tandem pairs was different in the absence of the dominant pol  $\eta$ , we examined sequences from  $Pol\zeta^{+/+} Pol\eta^{-/-}$  clones. Data were combined from approximately two-thirds immunized spleen cells (Fig. 2 A) and one-third Peyer's patch cells generated in this study, because there was no difference in SHM between the two populations. The location of 33 pairs of tandem substitutions and 1,060 single mutations were similar, and just 21% tandems occurred in WGCW hotspots (Fig. 3, C and D). Furthermore, only 40% tandems were located in 27 of the less stringent DGYW motifs (D = A/G/T, Y = C/T; Rogozin and Diaz, 2004). Thus, the majority of tandem pairs in wild-type and

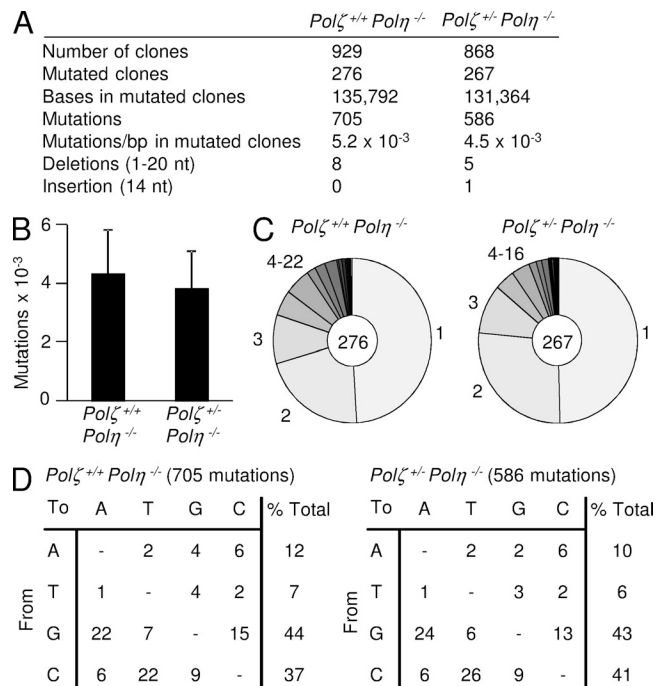


**Figure 2. Frequency and spectra of SHM in the J<sub>H</sub>4 intron from immunized spleen cells.** 10  $Pol\zeta^{+/+} Pol\eta^{-/-}$  (10 independent experiments with one mouse per experiment) or 12  $Pol\zeta^{+/-} Pol\eta^{-/-}$  (12 independent experiments with one mouse per experiment) littermate mice were immunized with NP<sub>36</sub>-CGG, and germinal center B cells were isolated 14 d later. SHM was analyzed in the J<sub>H</sub>4 intron downstream of rearranged V<sub>H</sub>J558 genes. (A) Summary of mutational data. (B) Mean frequency (mutations/base pair in mutated clones). (C) Distribution of mutations per clone. The number of mutated clones is shown in the center of each circle. Segments represent the proportion of clones that contain the indicated number of mutations. (D) Types of substitutions. The number of mutations is shown in parentheses. Mutations were recorded from the nontranscribed strand and have been corrected for base composition of the nucleotide sequence. Data are expressed as percentage of total mutations.

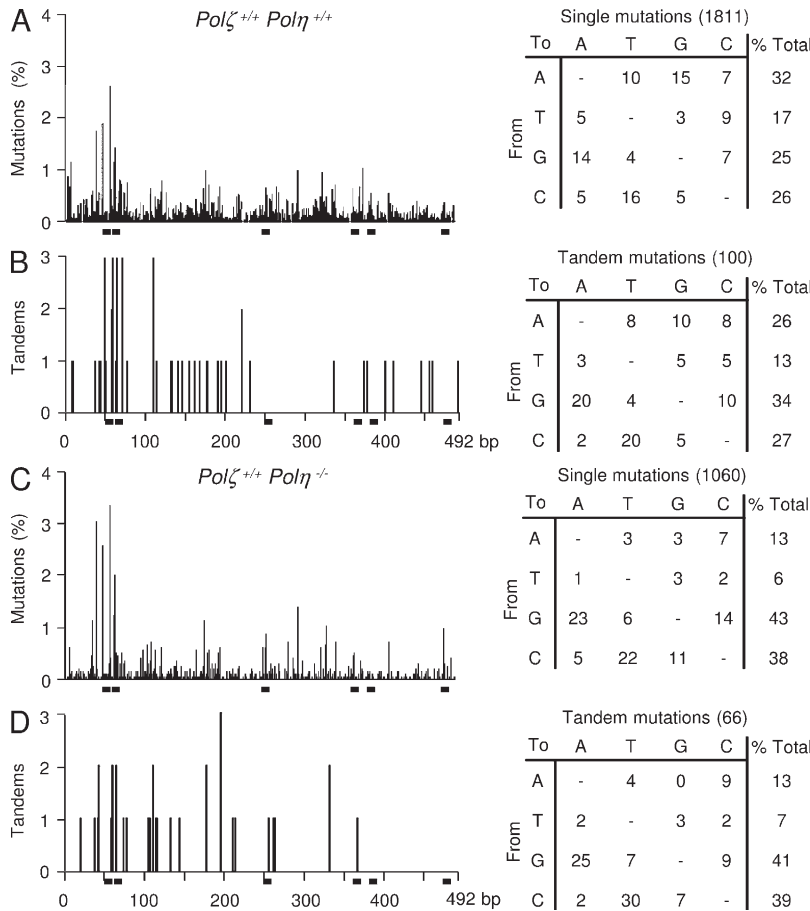


**Figure 3. Location and spectra of mutations in the J<sub>H</sub>4 intron from wild-type and *Polη*<sup>-/-</sup> mice.**

(A) Wild-type single mutations from published Peyer's patch cells and spleens immunized with NP<sub>36</sub>-CGG for 14 d. Sequencing data are plotted as percentage of 1811 mutations. Positions of WGCW hotspot motifs are represented by black bars on the abscissa. Substitutions have been corrected for base composition of the nucleotide sequence and are expressed as percentage of the mutations. (B) Wild-type tandem mutations. Position of 50 tandem pairs is plotted as absolute numbers. Substitutions at both tandem nucleotides have been corrected for base composition and are expressed as percentage of 100 tandem mutations. (C) *Polζ*<sup>+/+</sup> *Polη*<sup>-/-</sup> single mutations from Peyer's patch cells and spleens immunized with NP<sub>36</sub>-CGG for 14 d. Data are graphed as percentage of 1,060 mutations. (D) *Polζ*<sup>+/+</sup> *Polη*<sup>-/-</sup> tandem mutations. Data includes 33 tandem pairs; substitutions are expressed as percentage of 66 tandem mutations.

*pol η*-deficient mice were found outside of the hotspots, suggesting that they did not arise from multiple events targeting only these motifs.

Third, we analyzed sequences from *pol η*-deficient mice with one or two alleles of *pol ζ* to quantify the contribution of *pol ζ* to the tandem signature. Adjacent mutations could be produced by polymerases in a single event or sequentially after cell division. Using a calculation based on frequency and random distribution of mutations (Winter et al., 1998), the expected number of tandems increases as the number of mutations per clone increases, indicating that they can occur in multiple events (Michael et al., 2002). Table 1 lists the observed and expected number of adjacent mutations in clones from spleen and Peyer's patch cells. Notably, the majority of tandem mutations occurred in clones which had very few mutations (Table 1), further supporting the hypothesis that most tandems occur during a single event. The total observed values were compared with the total expected values and tested for significance using the Poisson distribution, as shown in Fig. 4 A. Tandem pairs were observed at a significantly higher frequency compared with the expected number in sequences from *Polζ*<sup>+/+</sup> *Polη*<sup>-/-</sup> ( $P < 10^{-7}$ ), *Polζ*<sup>+/-</sup> *Polη*<sup>-/-</sup> ( $P < 10^{-2}$ ), and wild-type *Polζ*<sup>+/+</sup> *Polη*<sup>+/+</sup> ( $P < 10^{-6}$ ) clones.

The ratio of observed to expected values was then determined, and was higher in *Polζ*<sup>+/+</sup> *Polη*<sup>-/-</sup> clones at 3.1 compared

with *Polζ*<sup>+/-</sup> *Polη*<sup>-/-</sup> clones at 2.5 (Fig. 4 A). The increase in contiguous mutations from clones with two copies of *pol ζ* compared with clones with one copy suggests that *pol ζ* is important for introducing tandem mutations into the *Ig* loci. Furthermore, the ratio in wild-type mice expressing the low-fidelity polymerases was lower at 2.2 compared with *pol η*-deficient clones. Because both *pol η* (Matsuda et al., 2001) and *pol ζ* have the capability to extend mismatches in vitro, and therefore potentially introduce contiguous mutations, the observa-

tion that the ratio in *Polζ*<sup>+/+</sup> *Polη*<sup>-/-</sup> clones was higher than in *Polζ*<sup>+/-</sup> *Polη*<sup>+/+</sup> clones suggests that most of these tandems are not introduced by *pol η*. Furthermore, the spectra of tandem mutations were similar to the single mutations (Fig. 3), which suggest that *pol ζ* can extend mismatched termini produced by other polymerases. In wild-type mice, *pol ζ* could extend mismatched termini produced by *pol η* (A/T bias),  $κ$  (A/T bias), Rev1 (C bias), and itself (no bias). In *pol η*-deficient mice, the overall single mutation spectra and the tandem spectra are decreased for A/T mutations because there are no *pol η*-generated mismatches. Thus, the first mutation has the signature of whatever polymerase is being used, and the second mutation produced by *pol ζ* will be random, because *pol ζ* does not have a strong substitution bias (Zhong et al., 2006).

To further confirm that *pol ζ* generated the tandem signature, sequences from *Polζ*<sup>+/-</sup> and *Polζ*<sup>-/-</sup> single cells from conditional knockout mice were analyzed (Schenten et al., 2009). Although there were fewer mutations in the single-cell analyses, the formula used to calculate the expected number of tandems takes into account the overall frequency of mutations per clone. The observed number of tandems was significantly higher than the expected number in *Polζ*<sup>+/-</sup> cells ( $P = 0.03$ ), but not in *Polζ*<sup>-/-</sup> cells ( $P = 0.35$ ). The *Polζ*<sup>+/-</sup> cells had a ratio of observed to expected tandems of 2.1,

**Table 1.** Observed and expected tandem mutations in pol  $\eta$ -deficient cells from spleen and Peyer's patches

Mutations per clone	<i>Pol<math>\zeta</math><sup>+/+</sup> Pol<math>\eta</math><sup>-/-</sup></i>				<i>Pol<math>\zeta</math><sup>+/-</sup> Pol<math>\eta</math><sup>-/-</sup></i>			
	No. of clones	No. of mutations	Tandems observed	Tandems expected <sup>a</sup>	No. of clones	No. of mutations	Tandems observed	Tandems expected <sup>a</sup>
1	157	157	0	0.00	140	140	0	0.00
2	76	152	3	0.31	77	154	1	0.30
3	34	102	5	0.41	33	99	0	0.40
4	19	76	3	0.46	13	52	4	0.32
5	19	95	5	0.77	11	55	0	0.45
6	9	54	3	0.55	4	24	0	0.24
7	9	63	1	0.77	4	28	2	0.34
8	11	88	4	1.25	4	32	1	0.46
9	5	45	0	0.73	1	9	0	0.15
10	3	30	1	0.55	3	30	1	0.55
11	3	33	1	0.67	0	0	0	0.00
12	2	24	0	0.54	0	0	0	0.00
13	3	39	3	0.95	0	0	0	0.00
14	3	42	0	1.11	1	14	0	0.37
15	4	60	4	1.71	0	0	0	0.00
Total:	357	1,060	33	10.78	291	637	9	3.58

<sup>a</sup>Expected tandems were calculated by the formula  $n(n-1)/k$  in a sequence of  $k$  nucleotides long containing  $n$  mutations (Winter et al., 1998).

whereas *Pol $\zeta$ <sup>-/-</sup>* cells had a lower ratio of 1.4. Therefore, in the complete absence of pol  $\zeta$ , the observed number of tandems was similar to the expected number, indicating that they arose by two separate events. This data, summarized in Fig. 4 B, supports the hypothesis that pol  $\zeta$  generates tandem mutations during SHM by extending mismatches produced by other polymerases. Slippage of polymerases on DNA templates also has the potential to produce multiple substitutions (Wilson et al., 1998), but the frequency of insertions and deletions in V genes is low, suggesting that this is not a major mechanism.

#### Mismatch repair promotes pol $\zeta$ access to DNA during SHM

There are two pathways that could allow synthesis by pol  $\zeta$  during SHM. In the UNG pathway, the polymerase could synthesize across abasic sites introduced by UNG removal of uracils. In the MSH2–MSH6 pathway, pol  $\zeta$  could synthesize in the gap produced by exonuclease 1. To determine which pathway is used by pol  $\zeta$ , we analyzed previously published sequences of the J<sub>H</sub>4 intron from *Ung<sup>-/-</sup>* (Rada et al., 2002), *Msh2<sup>-/-</sup>* (Frey et al., 1998), *Msh6<sup>-/-</sup>* (with new sequences added for this study; Martomo et al., 2004), and *Ung<sup>-/-</sup> Msh2<sup>-/-</sup>* clones (Rada et al., 2004). The observed number of tandems was significantly higher than the expected number in *Ung<sup>-/-</sup>* clones ( $P < 10^{-3}$ ), and the ratio of observed to expected tandems was 2.2, which was identical to the ratio seen in wild-type clones (Fig. 4, A and B). This indicates that pol  $\zeta$  is not introducing tandem substitutions in the UNG pathway. However, disruption of the mismatch repair proteins MSH2 and MSH6 decreased the observed number of tandem pairs, so there was no difference between observed and expected values ( $P = 0.19$ ). Mice deficient for both UNG and MSH2

also had no significant difference between observed and expected values ( $P = 0.12$ ). Thus, in the absence of MSH2 and MSH6, the ratio of observed to expected tandems was lower at 1.4, and in the combined absence of MSH2 and UNG, the

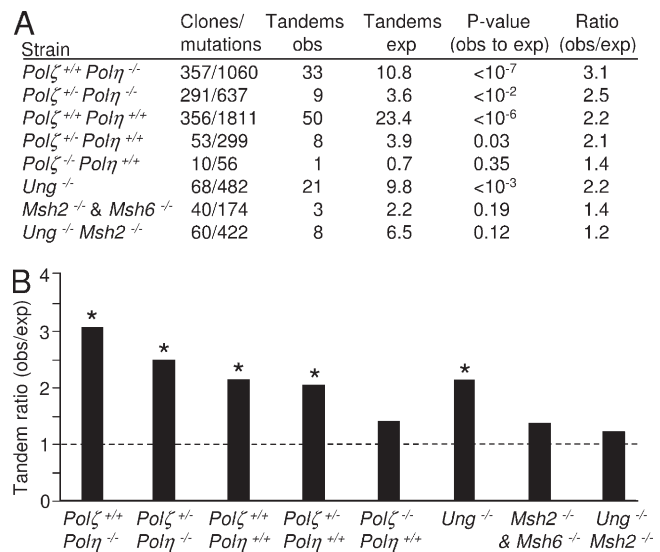


**Figure 4. More tandem mutations are introduced by pol  $\zeta$  in the absence of pol  $\eta$ .** (A) Tandem mutations in different strains. All data are from the J<sub>H</sub>4 intron, except *Pol $\zeta$ <sup>+/+</sup>* and *Pol $\zeta$ <sup>-/-</sup>* are from the J<sub>H</sub>1–4 introns. P values are based on Poisson calculations comparing the statistical difference between total observed and expected tandem mutations. (B) Tandem ratios in different strains. Dotted line indicates a ratio of 1 where observed and expected numbers are the same. \*, Observed tandems compared with expected tandems were significantly different ( $P \leq 0.03$ ).

ratio was 1.2. These results indicate that tandem mutations are produced more frequently in the MSH2–MSH6 pathway. The notion that pol  $\zeta$  might be used during mismatch repair is consistent with reports from yeast, where pol  $\zeta$  synthesis is reduced in mismatch repair-deficient strains (Lehner and Jinks-Robertson, 2009). One potential way pol  $\zeta$  could function during gap synthesis in SHM would be if another polymerase stalls after replicating over AID-induced uracils on the template strand to produce a A:U mismatch. Pol  $\zeta$  could then be recruited to extend the mispair and generate a second mispair. Additionally, pol  $\zeta$  could extend mismatched termini produced by other error-prone polymerases, i.e., pols  $\eta$ ,  $\kappa$ , or Rev1, and generate a second mispair. Because pol  $\zeta$  has no preferential mutational signature, both mechanisms will produce a spectra of tandems that matches the overall single mutation spectra as shown in Fig. 3.

A potential advantage of using pol  $\zeta$  to introduce contiguous mutations could be to more efficiently change amino acids in V genes to produce higher affinity. Codons are degenerate in the third base, and if two adjacent bases are changed simultaneously, the chance for an amino acid substitution is greater than with a single substitution. Interestingly, tandem mutations are found at extraordinary levels in nurse shark *Ig* genes (Zhu and Hsu, 2010), suggesting that nurse sharks may use pol  $\zeta$  more frequently than mice. Thus, our data support the participation of pol  $\zeta$  in SHM, and suggest that it has an increased role in the absence of the dominant pol  $\eta$  protein.

## MATERIALS AND METHODS

**Mice.** *Pol $\zeta$ <sup>+/-</sup>* mice on a mixed C57BL/6 X 129 background were obtained from J. Wittschleben and R. Wood (University of Texas, MD Anderson Cancer Center, Smithville, TX; Wittschleben et al., 2010) and bred to *Poh $\eta$ <sup>-/-</sup>* mice on a C57BL/6 background (Martomo et al., 2005). We have previously reported that SHM is identical in both the C57BL/6 and 129 strains of mice (McDonald et al., 2003). Genotypes were confirmed by PCR of tail DNA using *Rev3L<sup>+</sup>* and *Rev3L<sup>-</sup>* primer sets (Wittschleben et al., 2010) and *Poh $\eta$*  primer sets (Martomo et al., 2008). *Pol $\zeta$ <sup>+/-</sup> Poh $\eta$ <sup>-/-</sup>* mice were then bred to each other, which generated *Pol $\zeta$ <sup>+/+</sup> Poh $\eta$ <sup>-/-</sup>* mice and *Pol $\zeta$ <sup>+/-</sup> Poh $\eta$ <sup>-/-</sup>* mice. Littermate mice were used at 3–8 mo of age. All animal procedures were reviewed and approved by the Animal Care and Use Committee of the National Institute on Aging.

**RNA and proliferation assays.** Resting splenic B cells were isolated using negative selection with anti-CD43 and anti-CD11b magnetic beads (Miltenyi Biotec). For in vivo activation, mice were immunized with 100  $\mu$ g NP<sub>36</sub>-CGG (Biosearch Technologies) for 14 d. Splenic B cells were then stained with FITC-conjugated anti-B220 (SouthernBiotech) and Alexa Fluor 647-labeled anti-GL7 (eBioscience), and B220<sup>+</sup>GL7<sup>+</sup> cells were isolated by flow cytometry. RNA was isolated using RNeasy Mini kit (QIAGEN), and SuperScript III First-Strand Synthesis System for RT-PCR was used to prepare cDNA (Invitrogen). For quantitative real-time PCR, Power SYBR Green PCR Master Mix (Applied Biosystems) was used with the following primers: *Rev3* forward, 5'-GCTCAATGCCCGTCAACTAGGACTAAA-3' and reverse, 5'-CCAAGTCTCTCTGGCTTTGTGAAC-3'; *Rev7* forward, 5'-CTCGAAACATGGAGAAGATACAGGTCATCA-3' and reverse, 5'-AAATGTCCGACGTCATGGTTTTTAGGG-3'; *Rev1* forward, 5'-GGAAGAGAACGGAGAATGATGGCTGG-3' and reverse, 5'-GTTAGCAGCATCTGTGCGGAAGT-3'; *Pol $\eta$*  forward, 5'-GCAGACGGTCTTACTACCTGAAAGTTGTC-3' and reverse, 5'-CAGAAGTTCGAGACGCTTGGCAG-3'; *Pol $\kappa$*  forward,

5'-CAGTTAAACAACCCAAAGAAAGCTCGAGAAG-3' and reverse, 5'-CAAAGTTGAGCTCTTTGTCTTCGTTCTCCTG-3'; and  $\beta$ -*actin* primers (Saribasak et al., 2011). For proliferation, B cells were treated with 5  $\mu$ M CFSE (Invitrogen), incubated with LPS and IL-4 for 3 d, and analyzed by flow cytometry.

**CSR analysis.** Resting splenic B cells were plated at a density of 500,000 cells/ml and stimulated with 5  $\mu$ g/ml *Escherichia coli* LPS serotype 0111:B4 (Sigma-Aldrich) to induce switching to IgG3; LPS plus 5 ng/ml recombinant IL-4 (BD) to induce switching to IgG1; LPS plus 25 ng/ml IFN- $\gamma$  (R&D Systems) for switching to IgG2a; and LPS plus 2 ng/ml TGF- $\beta$  (R&D Systems) for IgG2b. After 4 d, the cells were stained with FITC-conjugated antibody to B220 along with phycoerythrin-conjugated antibodies to mouse IgG1, IgG2a, IgG2b, or IgG3 (SouthernBiotech) for analysis by flow cytometry.

**SHM analysis.** Mice were immunized by intraperitoneal injection of 100  $\mu$ g NP<sub>36</sub>-CGG (Biosearch Technologies) in adjuvant complex (Sigma-Aldrich). On day 14, splenic B cells were stained with FITC anti-B220 and Alexa Fluor anti-GL7. In nonimmunized mice, Peyer's patch B cells were also isolated and stained. B220<sup>+</sup> GL7<sup>+</sup> cells were isolated by flow cytometry, and DNA was prepared. The 492-bp intronic region downstream of J<sub>H</sub>4 from rearranged V<sub>H</sub>J558 genes was amplified by nested PCR. The first round used forward primer J558 5'-AGCCTGACATCTGAGGAC-3' and reverse primer JH2906 5'-GTGTTCCCTTGAAGCTGGAC-3', and the second round used forward primer J558Eco 5'-CCGGAATTCCTGACATCTGAGGACTCTGC-3' and reverse primer JH2827Bam 5'-CGCGGATCCGATGCCCTTCTCCCTTGACTC-3'. The amplified DNA was then digested with EcoRI and BamHI restriction enzymes, cloned into pBS-SK vector, and sequenced. Only clones with unique VDJ joins were scored.

**Online supplemental material.** Fig. S1 lists 101 sequences with tandem mutations in the J<sub>H</sub>4 intron and shows where they occur. Online supplemental material is available at <http://www.jem.org/cgi/content/full/jem.20112234/DC1>.

We thank Richard Wood and John Wittschleben for *Pol $\zeta$ <sup>+/-</sup>* mice; Klaus Rajewsky for sequence data; R. Wersto, C. Morris, J. Scheers, C. Nguyen, and T. Wolf for flow cytometry analyses; and Ranjan Sen and Kimberly Zanotti for valuable comments.

This research was supported entirely by the Intramural Research Program of the National Institutes of Health, National Institute on Aging.

The authors declare no competing financial interests.

Submitted: 21 October 2012

Accepted: 3 May 2012

## REFERENCES

- Bemark, M., A.A. Khamlichi, S.L. Davies, and M.S. Neuberger. 2000. Disruption of mouse polymerase zeta (Rev3) leads to embryonic lethality and impairs blastocyst development in vitro. *Curr. Biol.* 10:1213–1216. [http://dx.doi.org/10.1016/S0960-9822\(00\)00724-7](http://dx.doi.org/10.1016/S0960-9822(00)00724-7)
- Diaz, M., L.K. Verkoczy, M.F. Flajnik, and N.R. Klinman. 2001. Decreased frequency of somatic hypermutation and impaired affinity maturation but intact germinal center formation in mice expressing antisense RNA to DNA polymerase zeta. *J. Immunol.* 167:327–335.
- Eposito, G., I. Godindagger, U. Klein, M.L. Yaspo, A. Cumano, and K. Rajewsky. 2000. Disruption of the Rev3l-encoded catalytic subunit of polymerase zeta in mice results in early embryonic lethality. *Curr. Biol.* 10:1221–1224. [http://dx.doi.org/10.1016/S0960-9822\(00\)00726-0](http://dx.doi.org/10.1016/S0960-9822(00)00726-0)
- Faili, A., A. Stary, F. Delbos, S. Weller, S. Aoufouchi, A. Sarasin, J.C. Weill, and C.A. Reynaud. 2009. A backup role of DNA polymerase kappa in Ig gene hypermutation only takes place in the complete absence of DNA polymerase eta. *J. Immunol.* 182:6353–6359. <http://dx.doi.org/10.4049/jimmunol.0900177>
- Frey, S., B. Bertocci, F. Delbos, L. Quint, J.C. Weill, and C.A. Reynaud. 1998. Mismatch repair deficiency interferes with the accumulation of mutations in chronically stimulated B cells and not with the hypermutation process. *Immunity.* 9:127–134. [http://dx.doi.org/10.1016/S1074-7613\(00\)80594-4](http://dx.doi.org/10.1016/S1074-7613(00)80594-4)

- Hirano, Y., and K. Sugimoto. 2006. ATR homolog Mec1 controls association of DNA polymerase zeta-Rev1 complex with regions near a double-strand break. *Curr. Biol.* 16:586–590. <http://dx.doi.org/10.1016/j.cub.2006.01.063>
- Jansen, J.G., P. Langerak, A. Tsaalbi-Shtylik, P. van den Berk, H. Jacobs, and N. de Wind. 2006. Strand-biased defect in C/G transversions in hypermutating immunoglobulin genes in Rev1-deficient mice. *J. Exp. Med.* 203:319–323. <http://dx.doi.org/10.1084/jem.20052227>
- Johnson, R.E., M.T. Washington, L. Haracska, S. Prakash, and L. Prakash. 2000. Eukaryotic polymerases iota and zeta act sequentially to bypass DNA lesions. *Nature.* 406:1015–1019. <http://dx.doi.org/10.1038/35023030>
- Langerak, P., A.O. Nygren, P.H. Krijger, P.C. van den Berk, and H. Jacobs. 2007. A/T mutagenesis in hypermutated immunoglobulin genes strongly depends on PCNAK164 modification. *J. Exp. Med.* 204:1989–1998. <http://dx.doi.org/10.1084/jem.20070902>
- Lawrence, C.W., and V.M. Maher. 2001. Mutagenesis in eukaryotes dependent on DNA polymerase zeta and Rev1p. *Philos. Trans. R. Soc. Lond. B Biol. Sci.* 356:41–46. <http://dx.doi.org/10.1098/rstb.2000.0001>
- Lehner, K., and S. Jinks-Robertson. 2009. The mismatch repair system promotes DNA polymerase zeta-dependent translesion synthesis in yeast. *Proc. Natl. Acad. Sci. USA.* 106:5749–5754. <http://dx.doi.org/10.1073/pnas.0812715106>
- Martomo, S.A., W.W. Yang, and P.J. Gearhart. 2004. A role for Msh6 but not Msh3 in somatic hypermutation and class switch recombination. *J. Exp. Med.* 200:61–68. <http://dx.doi.org/10.1084/jem.20040691>
- Martomo, S.A., W.W. Yang, R.P. Wersto, T. Ohkumo, Y. Kondo, M. Yokoi, C. Masutani, F. Hanaoka, and P.J. Gearhart. 2005. Different mutation signatures in DNA polymerase eta- and MSH6-deficient mice suggest separate roles in antibody diversification. *Proc. Natl. Acad. Sci. USA.* 102:8656–8661. <http://dx.doi.org/10.1073/pnas.0501852102>
- Martomo, S.A., H. Saribasak, M. Yokoi, F. Hanaoka, and P.J. Gearhart. 2008. Reevaluation of the role of DNA polymerase theta in somatic hypermutation of immunoglobulin genes. *DNA Repair (Amst.)*. 7:1603–1608. <http://dx.doi.org/10.1016/j.dnarep.2008.04.002>
- Matsuda, T., K. Bebenek, C. Masutani, I.B. Rogozin, F. Hanaoka, and T.A. Kunkel. 2001. Error rate and specificity of human and murine DNA polymerase eta. *J. Mol. Biol.* 312:335–346. <http://dx.doi.org/10.1006/jmbi.2001.4937>
- Maul, R.W., and P.J. Gearhart. 2010. AID and somatic hypermutation. *Adv. Immunol.* 105:159–191. [http://dx.doi.org/10.1016/S0065-2776\(10\)05006-6](http://dx.doi.org/10.1016/S0065-2776(10)05006-6)
- Maul, R.W., H. Saribasak, S.A. Martomo, R.L. McClure, W. Yang, A. Vaisman, H.S. Gramlich, D.G. Schatz, R. Woodgate, D.M. Wilson III, and P.J. Gearhart. 2011. Uracil residues dependent on the deaminase AID in immunoglobulin gene variable and switch regions. *Nat. Immunol.* 12:70–76. <http://dx.doi.org/10.1038/ni.1970>
- McDonald, J.P., E.G. Frank, B.S. Plosky, I.B. Rogozin, C. Masutani, F. Hanaoka, R. Woodgate, and P.J. Gearhart. 2003. 129-derived strains of mice are deficient in DNA polymerase iota and have normal immunoglobulin hypermutation. *J. Exp. Med.* 198:635–643. <http://dx.doi.org/10.1084/jem.20030767>
- Michael, N., T.E. Martin, D. Nicolae, N. Kim, K. Padjen, P. Zhan, H. Nguyen, C. Pinkert, and U. Storb. 2002. Effects of sequence and structure on the hypermutability of immunoglobulin genes. *Immunity.* 16:123–134. [http://dx.doi.org/10.1016/S1074-7613\(02\)00261-3](http://dx.doi.org/10.1016/S1074-7613(02)00261-3)
- Petersen-Mahrt, S.K., R.S. Harris, and M.S. Neuberger. 2002. AID mutates *E. coli* suggesting a DNA deamination mechanism for antibody diversification. *Nature.* 418:99–103. <http://dx.doi.org/10.1038/nature00862>
- Rada, C., G.T. Williams, H. Nilsen, D.E. Barnes, T. Lindahl, and M.S. Neuberger. 2002. Immunoglobulin isotype switching is inhibited and somatic hypermutation perturbed in UNG-deficient mice. *Curr. Biol.* 12:1748–1755. [http://dx.doi.org/10.1016/S0960-9822\(02\)01215-0](http://dx.doi.org/10.1016/S0960-9822(02)01215-0)
- Rada, C., J.M. Di Noia, and M.S. Neuberger. 2004. Mismatch recognition and uracil excision provide complementary paths to both Ig switching and the A/T-focused phase of somatic mutation. *Mol. Cell.* 16:163–171. <http://dx.doi.org/10.1016/j.molcel.2004.10.011>
- Roa, S., E. Avdievich, J.U. Peled, T. Maccarthy, U. Werling, F.L. Kuang, R. Kan, C. Zhao, A. Bergman, P.E. Cohen, et al. 2008. Ubiquitylated PCNA plays a role in somatic hypermutation and class-switch recombination and is required for meiotic progression. *Proc. Natl. Acad. Sci. USA.* 105:16248–16253. <http://dx.doi.org/10.1073/pnas.0808182105>
- Rogozin, I.B., and M. Diaz. 2004. Cutting edge: DGYW/WRCH is a better predictor of mutability at G:C bases in Ig hypermutation than the widely accepted RGYW/WRCY motif and probably reflects a two-step activation-induced cytidine deaminase-triggered process. *J. Immunol.* 172:3382–3384.
- Sakamoto, A.N., J.E. Stone, G.E. Kissling, S.D. McCulloch, Y.I. Pavlov, and T.A. Kunkel. 2007. Mutator alleles of yeast DNA polymerase zeta. *DNA Repair (Amst.)*. 6:1829–1838. <http://dx.doi.org/10.1016/j.dnarep.2007.07.002>
- Saribasak, H., R.W. Maul, Z. Cao, R.L. McClure, W. Yang, D.R. McNeill, D.M. Wilson III, and P.J. Gearhart. 2011. XRCC1 suppresses somatic hypermutation and promotes alternative nonhomologous end joining in Igh genes. *J. Exp. Med.* 208:2209–2216. <http://dx.doi.org/10.1084/jem.20111135>
- Schenten, D., S. Kracker, G. Esposito, S. Franco, U. Klein, M. Murphy, F.W. Alt, and K. Rajewsky. 2009. Pol zeta ablation in B cells impairs the germinal center reaction, class switch recombination, DNA break repair, and genome stability. *J. Exp. Med.* 206:477–490. <http://dx.doi.org/10.1084/jem.20080669>
- Seki, M., P.J. Gearhart, and R.D. Wood. 2005. DNA polymerases and somatic hypermutation of immunoglobulin genes. *EMBO Rep.* 6:1143–1148. <http://dx.doi.org/10.1038/sj.embor.7400582>
- Wilson, P.C., O. de Bouteiller, Y.J. Liu, K. Potter, J. Banchereau, J.D. Capra, and V. Pascual. 1998. Somatic hypermutation introduces insertions and deletions into immunoglobulin V genes. *J. Exp. Med.* 187:59–70. <http://dx.doi.org/10.1084/jem.187.1.59>
- Winter, D.B., Q.H. Phung, A. Umar, S.M. Baker, R.E. Tarone, K. Tanaka, R.M. Liskay, T.A. Kunkel, V.A. Bohr, and P.J. Gearhart. 1998. Altered spectra of hypermutation in antibodies from mice deficient for the DNA mismatch repair protein PMS2. *Proc. Natl. Acad. Sci. USA.* 95:6953–6958. <http://dx.doi.org/10.1073/pnas.95.12.6953>
- Wittschieben, J., M.K. Shivji, E. Lalani, M.A. Jacobs, F. Marini, P.J. Gearhart, I. Rosewell, G. Stamp, and R.D. Wood. 2000. Disruption of the developmentally regulated Rev3l gene causes embryonic lethality. *Curr. Biol.* 10:1217–1220. [http://dx.doi.org/10.1016/S0960-9822\(00\)00725-9](http://dx.doi.org/10.1016/S0960-9822(00)00725-9)
- Wittschieben, J.P., V. Patil, V. Glushets, L.J. Robinson, D.F. Kusewitt, and R.D. Wood. 2010. Loss of DNA polymerase zeta enhances spontaneous tumorigenesis. *Cancer Res.* 70:2770–2778. <http://dx.doi.org/10.1158/0008-5472.CAN-09-4267>
- Zan, H., A. Komori, Z. Li, A. Cerutti, A. Schaffer, M.F. Flajnik, M. Diaz, and P. Casali. 2001. The translesion DNA polymerase zeta plays a major role in Ig and bcl-6 somatic hypermutation. *Immunity.* 14:643–653. [http://dx.doi.org/10.1016/S1074-7613\(01\)00142-X](http://dx.doi.org/10.1016/S1074-7613(01)00142-X)
- Zeng, X., D.B. Winter, C. Kasmer, K.H. Kraemer, A.R. Lehmann, and P.J. Gearhart. 2001. DNA polymerase eta is an A-T mutator in somatic hypermutation of immunoglobulin variable genes. *Nat. Immunol.* 2:537–541. <http://dx.doi.org/10.1038/88740>
- Zhong, X., P. Garg, C.M. Stith, S.A. Nick McElhinny, G.E. Kissling, P.M. Burgers, and T.A. Kunkel. 2006. The fidelity of DNA synthesis by yeast DNA polymerase zeta alone and with accessory proteins. *Nucleic Acids Res.* 34:4731–4742. <http://dx.doi.org/10.1093/nar/gkl465>
- Zhu, C., and E. Hsu. 2010. Error-prone DNA repair activity during somatic hypermutation in shark B lymphocytes. *J. Immunol.* 185:5336–5347. <http://dx.doi.org/10.4049/jimmunol.1000779>